

# Europium–Hydrogen Bond Distances in Saline Metal Hydrides by Neutron Diffraction

Klaus Yvon\*, Holger Kohlmann, and Bernard Bertheville

**Abstract.** Europium–hydrogen bond distances in saline metal hydrides have been refined from neutron powder diffraction data on the magnesium-based ternary deuterides  $\text{EuMg}_2\text{D}_6$ ,  $\text{EuMgD}_4$ ,  $\text{Eu}_2\text{MgD}_6$ ,  $\text{Eu}_6\text{Mg}_7\text{D}_{26}$  and  $\text{Eu}_2\text{Mg}_3\text{D}_{10}$ . Absorption effects were attenuated by choosing neutron energies close to the minimum absorption cross section of natural isotope mixtures of europium and by using annular sample holders on high-flux neutron diffractometers. Some structures required joint refinements of neutron and synchrotron diffraction data. The Eu–D distances found for the various coordination numbers of europium range between 237–276 pm (CN=9), 220–287 pm (CN=10), 239–287 pm (CN=11) and 228–299 pm (CN=12). They are closely similar to, but shorter by about 4 pm than the corresponding Sr–D distances in strontium analogues, thus underlining the analogy between the europium and alkaline-earth hydride chemistry.

**Keywords:** Crystal structures · Metal hydrides · Neutron diffraction · Rare-earth compounds · Synchrotron X-ray diffraction

## 1. Introduction

Until recently crystal structures of europium-based ternary metal hydrides were virtually unknown and no reliable values existed for interatomic Eu–H distances. The main reason for this lack of knowledge is the extremely high absorption cross section of natural isotope mixtures of europium for thermal neutrons. Neutron diffraction experiments are essential to define hydrogen atom positions in metal hydride structures to a satisfactory precision. Another reason is the absence of suitable single crystals, which means that the crystal structures have to be solved from powder diffraction data. This more cumbersome method relies on single-phase samples that are not always available in sufficient quantities. Finally, the relatively low symmetry and complexity of most metal hydride structures caused additional difficulties. The present paper shows how some of these dif-

ficulties can be overcome by optimising the experimental set-up of the diffraction methods and by choosing suitable structure refinement procedures. Results obtained on ternary europium-magnesium-hydride structures will be summarised and compared with those recently obtained for alkaline earth analogues. The data complete the crystal chemistry of divalent metal hydrides and are useful for a better understanding of the europium–hydrogen interactions in the solid state.

## 2. Experimental

### 2.1. Synthesis

In view of the unfavourable cross-section of hydrogen for thermal neutrons, deuterated samples were prepared. For economic reasons natural isotope mixtures of europium ( $^{151}\text{Eu}$ , containing strongly neutron absorbing  $^{151}\text{Eu}$ ) rather than the less absorbing (but exceedingly expensive)  $^{153}\text{Eu}$  were used. Six metal deuterides belonging to the ternary europium-magnesium-deuterium system were investigated. While some ( $\text{EuD}_2$ ,  $\text{EuMg}_2\text{D}_6$ ,  $\text{EuMgD}_4$ ) were prepared by deuteration of the elements or binary metal alloys in an autoclave at temperatures of 600 K and deuterium gas pressures of up to 50

bar [1][2], others ( $\text{Eu}_2\text{MgD}_6$ ,  $\text{Eu}_6\text{Mg}_7\text{D}_{26}$ ,  $\text{Eu}_2\text{Mg}_3\text{D}_{10}$ ) were prepared by solid-state reactions from mixtures of the binary metal hydrides in a multi-anvil press at quasi-hydrostatic pressures of up to 3.5 GPa and temperatures of up to 870 K [3]. The reaction products obtained were all coloured. They were moisture sensitive and needed to be handled in an argon-filled glove box. Some were investigated magnetically. The range of measured effective magnetic moments ( $\mu_{\text{eff}} = 7.54\text{--}8.12\mu_{\text{B}}$ ) was consistent with the presence of divalent europium (free  $\text{Eu}^{2+}$  ion:  $7.95\mu_{\text{B}}$ ). The size of the polycrystalline samples was of the order of  $1\text{ cm}^3$ . Most samples were multiphase and contained significant amounts of non-reacted  $\text{EuD}_2$  and  $\text{MgD}_2$  and impurity phases (mainly  $\text{MgO}$ ). Single crystals of adequate size were not found.

### 2.2. Diffraction Experiments

Natural isotope mixtures of europium consist of almost equal amounts of  $^{151}\text{Eu}$  and  $^{153}\text{Eu}$  and have neutron absorption cross sections ( $\sigma_a = 4530$  barns at  $\lambda = 179.8$  pm [4]) that exceed that of the shielding material cadmium. In order to attenuate this effect for the diffraction experiments the following measures were taken. Firstly, a neutron wavelength

\*Correspondence: Prof. Dr. K. Yvon  
Laboratoire de Cristallographie,  
Université de Genève  
24 Quai Ernest Ansermet,  
CH-1211 Genève 4  
Tel.: +41 22 702 6231  
Fax: +41 22 702 6864  
E-Mail: Klaus.Yvon@cryst.unige.ch

near the minimum of the energy-dependent absorption cross section of  $^{nat}\text{Eu}$  was chosen. As shown in Fig. 1 this minimum is situated near  $\lambda = 73$  pm and  $\sigma_a = 860$  barns. The wavelength dependency of  $\sigma_a$  was calculated according to the relation  $\sigma_a = 4\pi b_c''/k$  ( $k$ =neutron wave vector;  $b_c''$ =imaginary part of coherent scattering length [5]).

This measure allowed the transmission factor of the samples to be increased by more than one order of magnitude at low diffraction angles. Secondly, the commonly used single-walled cylindrical sample containers were replaced by double-walled containers made of vanadium. As shown in Fig. 2 this allowed the transmission to be further increased by a factor of up to seven, thus leading to a total intensity gain of up to two orders of magnitude. The graphs in Fig. 2 were calculated by ABSOR [6] for binary  $\text{EuD}_2$  (linear absorption coefficient  $\mu = 20.67$   $\text{cm}^{-1}$  at  $\lambda = 70$  pm, 50% packing density) by assuming a sample of given volume filling either a single-walled cylinder (inner diameter 0.45 cm) or a double-walled cylinder (inner diameter of outer cylinder 0.915 cm, outer diameter of inner cylinder 0.796 cm, annular sample thickness  $\sim 0.06$  cm). Similar graphs were obtained for the ternary deuteride phases ( $\mu = 8.1$   $\text{cm}^{-1}$  for  $\text{EuMg}_2\text{D}_6$  and  $12.5$   $\text{cm}^{-1}$  for  $\text{EuMgD}_4$  at  $\lambda = 80.45$  pm;  $15.6$   $\text{cm}^{-1}$  for  $\text{Eu}_2\text{MgD}_6$ ,  $11.4$   $\text{cm}^{-1}$  for  $\text{Eu}_6\text{Mg}_7\text{D}_{26}$  and  $10.1$   $\text{cm}^{-1}$  for  $\text{Eu}_2\text{Mg}_3\text{D}_{10}$  at  $\lambda = 70.50$  pm). Finally, the high intensity powder diffractometers D20 (equipped with a position sensitive detector) and D4b (installed on a hot source) at the high-flux reactor of the Institute Laue-Langevin (Grenoble, France) were used. Data collection times ranged between 6 and 32 h.

X-ray diffraction experiments were performed on both a laboratory source (CoK $\alpha$  or CuK $\alpha$  radiation) and a synchrotron radiation facility. High resolution was necessary for certain hydride structures because they showed a lowering of their lattice symmetry that was not detected on the laboratory X-ray source (see below). For this purpose the samples were enclosed in sealed glass capillaries (0.02 cm outer diameter) and mounted on the powder diffractometer of the Swiss-Norwegian beamline (BM1B) at the European Synchrotron Radiation Facility (Grenoble, France). The samples came from the same batches as those investigated by neutron diffraction. Measurements were performed in the angular range  $3^\circ \leq 2\theta \leq 43^\circ$  with a step size of  $\Delta 2\theta = 0.005^\circ$  at a wavelength of  $\lambda = 60.054(1)$  pm during 6 h.

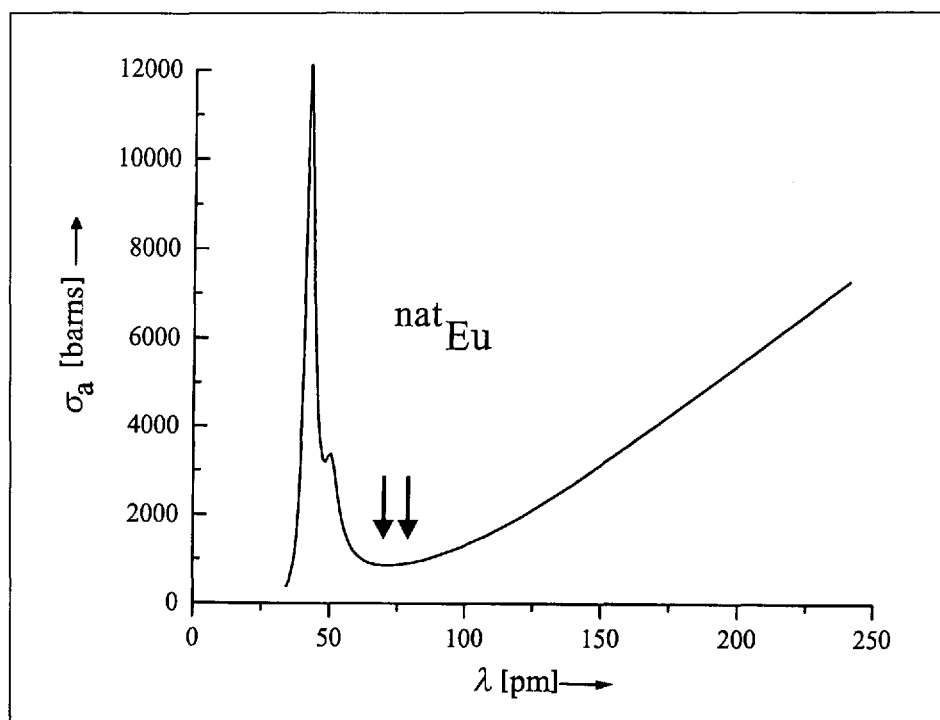


Fig. 1. Absorption cross section of a natural isotope mixture of europium for neutrons as a function of wavelength (adapted from Fig. 1 in [1]). Arrows indicate the wavelengths used for the neutron diffraction experiments ( $\lambda = 80.45$  and  $70.5$  pm).

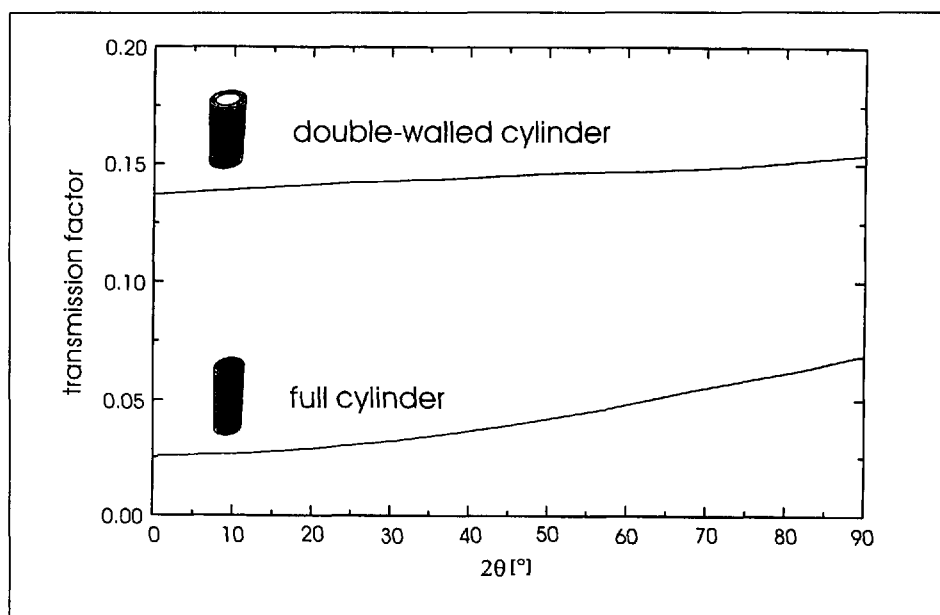


Fig. 2. Transmission factors calculated for a single-walled and a double-walled vanadium cylinder filled with  $\text{EuD}_2$  powders having the same volume (for details see text).

### 2.3. Structure Solution and Refinement

Most structures were solved *ab-initio* by taking advantage of the strong scattering contrast of the constituting elements for X-rays and neutrons. Complications arose due to the structural complexity (up to 16 symmetry independent atom sites), pseudo-symmetry ( $\text{EuMgD}_4$ ) and lattice distortions ( $\text{Eu}_6\text{Mg}_7\text{D}_{26}$ ). For structure refinement standard Rietveld programmes capable of performing multi-phase and joint refinements on different

diffraction patterns were used [7][8]. While some refinements ( $\text{EuD}_2$ ,  $\text{EuMg}_2\text{D}_6$ ,  $\text{EuMgD}_4$ ) gave satisfactory results during consecutive refinement steps (first on X-ray data, then on neutron data) others ( $\text{Eu}_2\text{MgD}_6$ ,  $\text{Eu}_6\text{Mg}_7\text{D}_{26}$ ,  $\text{Eu}_2\text{Mg}_3\text{D}_{10}$ ) gave satisfactory fits and accurate metal positions only for the synchrotron data, but unstable refinements and inaccurate deuterium positions for the neutron data, even when applying severe constraints. In order to make use of the complementary nature of both types

of data, a joint structure refinement was performed by simultaneous use of five data sets (two synchrotron, three neutron patterns) collected on three samples. Up to eight phases were refined by using a recent version of GSAS [8] that allowed the imaginary part of the neutron scattering length,  $b''$ , of  $^{151}\text{Eu}$  to be included. The joint refinement converged and yielded structure parameters of satisfactory precision (for details see [3]). Absorption corrections were applied for the synchrotron data according to Hewat's formula [9] and for the neutron data by calculating transmission factors for annular samples by using the programme ABSOR [6]. As expected, these corrections did not change the atomic parameters significantly, except for a 15% increase of the atomic displacement amplitudes. For the ternary phases the (isotropic) displacement amplitudes were constrained to be equal for atoms of the same kind. In the final refinement up to 182 parameters were refined (60 positional, 11 thermal displacement, 20 cell, one preferred orientation for  $\text{Eu}_2\text{MgD}_6$  in the synchrotron data by the March-Dollase model [10], 36 background parameters, 33 phase fractions and 21 profile parameters). It is worth pointing out that absorption effects in the neutron data were still appreciable despite the use of a suitable wavelength and annular sample holders. As a result the accuracy of the structure parameters did not reach the standard of other metal

hydride structures, but was sufficient for the purpose of discussing the crystal chemistry (see below).

### 3. Results

The europium hydrides covered in this work are saline and can be rationalized in terms of divalent metal cations ( $\text{Eu}^{2+}$ ,  $\text{Mg}^{2+}$ ) and hydride anions ( $\text{H}^-$ ). Of particular interest for the understanding of the europium-hydrogen interactions are the hydrogen coordinations around the europium sites together with the corresponding Eu-H bond lengths. For this purpose, coordination numbers (CNs) were defined by assuming a cut-off value for Eu-D distances in the deuterides of 300 pm, the next longest Eu-D distances being generally >320 pm. As to the metal-hydrogen distances they can be assumed to be about 0.4 pm longer, on the average, than the corresponding metal-deuteride distances. As shown by the graphical representations of the coordination polyhedra in Fig. 3 and the list of Eu-D distances in Table 1 europium adopts the CNs = 9, 10, 11 and 12. Clearly, for a given CN, both the shapes and the Eu-D distances of the coordination polyhedra vary considerably from one deuteride structure to another. The average Eu-D distances tend to increase as the CNs of europium increase. The lowest coordination number (CN=9) and

shortest average Eu-D distances occur in binary  $\text{EuD}_2$  (tri-capped trigonal prism,  $\langle\text{Eu-D}\rangle=255$  pm) and ternary  $\text{EuMgD}_4$  (trigonal prism having two faces capped by three ligands,  $\langle\text{Eu-D}\rangle=252$  pm). Intermediate coordination numbers (CN=10 and 11) and Eu-D distances occur in  $\text{Eu}_6\text{Mg}_7\text{D}_{26}$  (Eu1: CN=10,  $\langle\text{Eu-D}\rangle=257$  pm; Eu1': CN=11,  $\langle\text{Eu-D}\rangle=264$  pm) that derive from a barium site (CN=12) in the higher symmetric barium analogue (see below). The highest coordination numbers (CN=12) and longest average Eu-D distances occur in  $\text{EuMg}_2\text{H}_6$  (cuboctahedron,  $\langle\text{Eu-D}\rangle=258$  pm),  $\text{Eu}_2\text{Mg}_3\text{H}_{10}$  (Eu1: twinned cuboctahedron,  $\langle\text{Eu-D}\rangle=271$  pm; Eu2: cuboctahedron,  $\langle\text{Eu-D}\rangle=265$  pm), and  $\text{Eu}_2\text{MgH}_6$  (twinned cuboctahedron,  $\langle\text{Eu-D}\rangle=264$  pm). Cuboctahedra of similar size are also found in the salt-like  $\text{EuLiD}_3$  ( $\langle\text{Eu-D}\rangle=268$  pm [2]) and the presumably metallic  $\text{EuPdD}_3$  ( $\langle\text{Eu-D}\rangle=269$  pm [12]). As to the magnesium atom environment all structures contain distorted  $\text{MgH}_6$  octahedra that are either isolated ( $\text{Eu}_2\text{MgH}_6$ ) or share corners ( $\text{EuMgH}_4$ ,  $\text{EuMg}_2\text{H}_6$ ) or edges and corners ( $\text{Eu}_6\text{Mg}_7\text{H}_{26}$ ,  $\text{Eu}_2\text{Mg}_3\text{H}_{10}$ ). The D-D distances are all longer than 200 pm and thus consistent with repulsive D-D interactions.

Given the similarities between the structure chemistry of divalent europium and alkaline earth elements, a comparison of their hydride structures is of interest. As shown in Table 2 all europium

Table 1. Eu-D distances<sup>a)</sup> (pm) and deuterium coordination numbers CN<sup>b)</sup> for europium-based metal hydrides, and comparison with corresponding Sr-D distances in strontium analogues (in *italics*).

Compound CN (Eu, Sr)= (structure type, space group)	9	10	11	12
<b>EuD<sub>2</sub></b> ( $\text{PbCl}_2$ , $Pnma$ ) [2] <i>SrD<sub>2</sub></i> [11]	238–276 <255>	243–281 <260>		
<b>Eu<sub>2</sub>MgD<sub>6</sub></b> ( $\text{K}_2\text{GeF}_6$ , $P\bar{3}m1$ ) [3] <i>Sr<sub>2</sub>MgD<sub>6</sub></i> [20]				251–276 <264> 250–278 <265>
<b>EuMgD<sub>4</sub></b> ( $\text{BaZnF}_4$ , $Cmc2_1$ ) [1] <i>SrMgD<sub>4</sub></i> [16]	237–270 <252>	243–282 <257>		
<b>Eu<sub>6</sub>Mg<sub>7</sub>D<sub>26</sub></b> ( $\text{Ba}_6\text{Zn}_7\text{F}_{26}$ , $I2/m$ ) [3]		Eu1: 243–284 <257> Eu2: 220–287 <256>	Eu1': 239–287 <264>	
<b>Eu<sub>2</sub>Mg<sub>3</sub>D<sub>10</sub></b> ( $\text{Ba}_2\text{Ni}_3\text{F}_{10}$ , $C2/m$ ) [3] <i>Sr<sub>2</sub>Mg<sub>3</sub>D<sub>10</sub></i> [13]				Eu1: 228–299 <271> Eu2: 229–289 <265> Sr1: 249–296 <274> Sr2: 251–289 <270>
<b>EuMg<sub>2</sub>D<sub>6</sub></b> ( $\text{EuMg}_2\text{D}_6$ , $P4/mmm$ ) [1]				254–266 <258>
average Eu-D distances	253	257	264	263

<sup>a)</sup> minimum, maximum and <average> Eu-D distances; e.s.d.'s of Eu compounds are typically <3 pm and of Sr compound <1 pm,

<sup>b)</sup> calculated by assuming a cut-off value of Eu-D=300 pm; for ligand geometries see Fig. 3.

hydrides except  $\text{EuMg}_2\text{H}_6$  have alkaline earth analogues. Of particular interest are the strontium members because the crystal radii of  $\text{Sr}^{2+}$  (145, 150 and 158 pm for CNs 9, 10 and 12, respectively [24]) are close to those of  $\text{Eu}^{2+}$  (144 and 149 pm for CNs 9 and 10, respectively [24]). This is confirmed by the structure data which show that all strontium-based hydride structures are strictly isotypic with the corresponding europium-based hydride structures, and that the Eu–D distances are very similar to, but shorter by about 4 pm, on average, than the corre-

sponding Sr–D distances. On the other hand, the barium structures are not all strictly isotypic with the corresponding europium and strontium structures. This is presumably due to the relatively large crystal radii of  $\text{Ba}^{2+}$  (161, 166 and 175 pm for CNs 9, 10 and 12, respectively [24]) compared to  $\text{Eu}^{2+}$  and  $\text{Sr}^{2+}$  that favours bigger CNs. In fact, while  $\text{Eu}_2\text{MgH}_6$  and  $\text{Eu}_2\text{Mg}_3\text{H}_{10}$  have the same crystal symmetry and CNs as the corresponding barium compounds, monoclinic  $\text{Eu}_6\text{Mg}_7\text{H}_{26}$  has fundamentally different cation coordinations compared to its

orthorhombic barium analogue. Specifically, the coordination polyhedra around Eu1 and Eu2 derive from the corresponding cuboctahedra in  $\text{Ba}_6\text{Mg}_7\text{D}_{26}$  by removal of two ligands, and that around Eu1' by removal of two ligands and the addition of one ligand. Note that synchrotron data were essential to detect the symmetry lowering in the europium structure. Neutron data alone would have yielded CN=12 for the europium sites and strongly biased Eu–D distances. Significant differences between Eu(Sr) and Ba coordinations also occur in non-centrosymmetric  $\text{EuMgH}_4$  (CN=9) compared to its centrosymmetric barium analogue (CN=11). The absence of inversion symmetry in the former structure was only revealed by the neutron data.

Finally, in contrast to the strontium and barium analogues, no calcium analogues for europium and strontium appear to exist in this structure family. This is presumably due to the relatively small crystal radius of  $\text{Ca}^{2+}$  (132, 137 and 148 pm for CNs 9, 10 and 12, respectively [24]) compared to those of  $\text{Eu}^{2+}$  and  $\text{Sr}^{2+}$ . On the other hand, the existence of hydride analogues between calcium and ytterbium suggests that divalent  $\text{Yb}^{2+}$  has a similar crystal radius as  $\text{Ca}^{2+}$ . Altogether the results suggest that atomic size effects play a major role for the structural stability of these hydride structures.

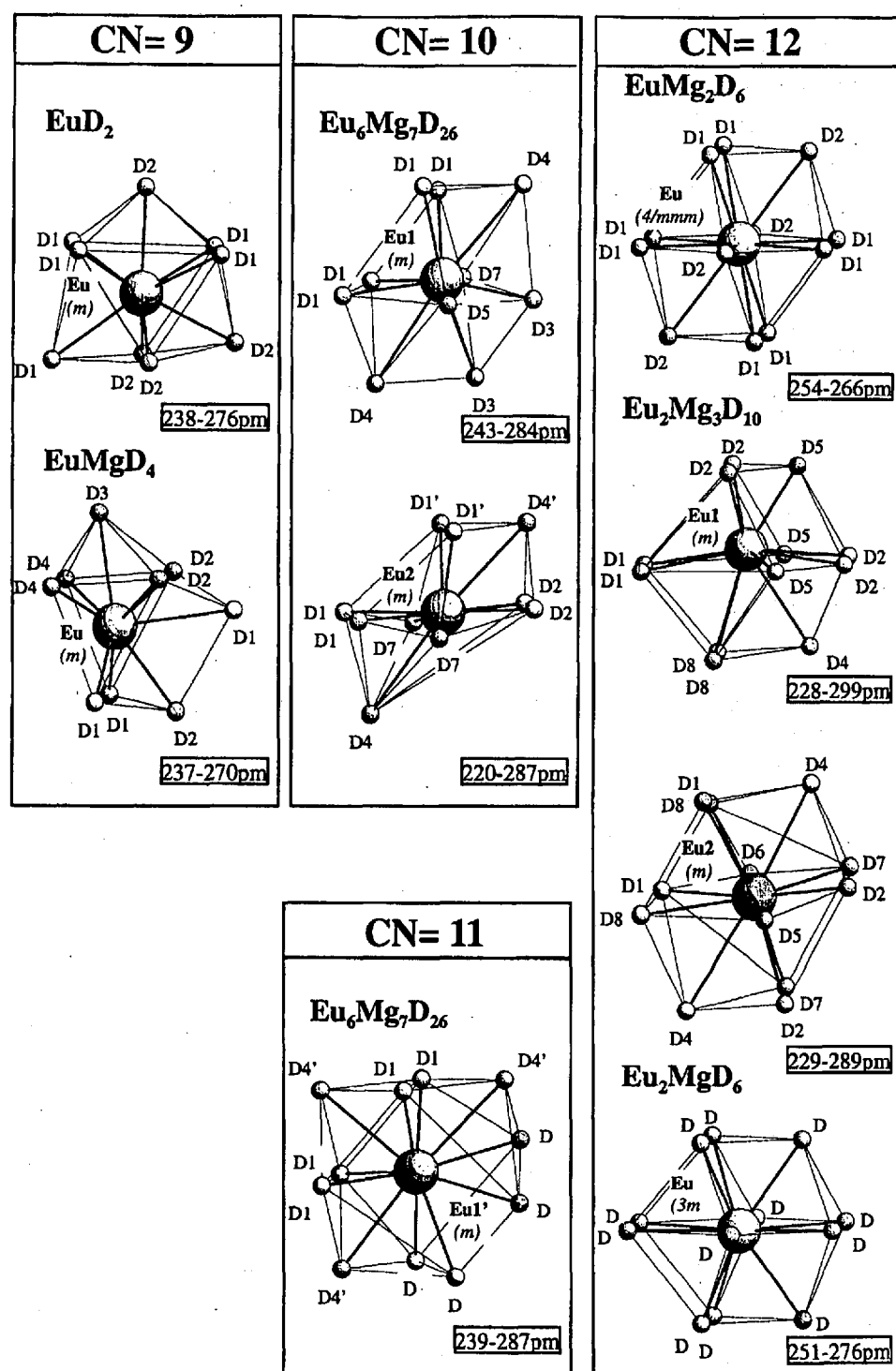


Fig. 3. Coordination polyhedra around europium in ternary europium-magnesium-deuterides. Point symmetries indicated in italics, atom labels according to [1–3]. Inserts: maximum and minimum Eu–D distances.

Table 2. Ternary europium-magnesium hydrides and comparison with alkaline earth and ytterbium analogues<sup>a)</sup>

Ca	Sr	Ba	Eu	Yb	structure type space group
			<b>EuMg<sub>2</sub>H<sub>6</sub></b> <sup>[1]</sup>		EuMg <sub>2</sub> H <sub>6</sub> P4/mmm
	Sr <sub>2</sub> Mg <sub>3</sub> H <sub>10</sub> <sup>[13]</sup>	Ba <sub>2</sub> Mg <sub>3</sub> H <sub>10</sub> <sup>[14]</sup>	<b>Eu<sub>2</sub>Mg<sub>3</sub>H<sub>10</sub></b> <sup>[3]</sup>		Ba <sub>2</sub> Ni <sub>3</sub> F <sub>10</sub> C2/m
			<b>Eu<sub>6</sub>Mg<sub>7</sub>H<sub>26</sub></b> <sup>[3]</sup>		Ba <sub>6</sub> Zn <sub>7</sub> F <sub>26</sub> C 2/m
		Ba <sub>6</sub> Mg <sub>7</sub> H <sub>26</sub> <sup>[15]</sup>			Ba <sub>6</sub> Mg <sub>7</sub> H <sub>26</sub> I mmm
	SrMgH <sub>4</sub> <sup>[16]</sup>		<b>EuMgH<sub>4</sub></b> <sup>[1]</sup>		BaZnF <sub>4</sub> Cmc2 <sub>1</sub>
		BaMgH <sub>4</sub> <sup>[17]</sup>			LaNiH <sub>4</sub> Cmcm
Ca <sub>4</sub> Mg <sub>3</sub> H <sub>14</sub> <sup>[18]</sup>				Yb <sub>4</sub> Mg <sub>3</sub> H <sub>14</sub> <sup>[19]</sup>	Ca <sub>4</sub> Mg <sub>3</sub> H <sub>14</sub> P-62m
	Sr <sub>2</sub> MgH <sub>6</sub> <sup>[20]</sup>	Ba <sub>2</sub> MgH <sub>6</sub> <sup>[21]</sup>	<b>Eu<sub>2</sub>MgH<sub>6</sub></b> <sup>[3]</sup>		K <sub>2</sub> GeF <sub>6</sub> P-3m1
Ca <sub>19</sub> Mg <sub>8</sub> H <sub>54</sub> <sup>[22]</sup>				Yb <sub>19</sub> Mg <sub>8</sub> H <sub>54</sub> <sup>[23]</sup>	Yb <sub>19</sub> Mg <sub>8</sub> H <sub>54</sub> Im-3

<sup>a)</sup> arranged in decreasing Mg content, all compounds (except Ba<sub>2</sub>MgH<sub>6</sub>) synthesized in Geneva

#### 4. Conclusions

The structural and magnetic properties of the ternary europium hydrides covered in this work are consistent with their description as ionic hydrides containing divalent europium. All compounds have alkaline earth analogues thus underlining the similarity between the europium and alkaline earth hydride chemistry. The metal hydrogen bond distances show that the atomic radius of divalent europium in saline metal hydrides is about 4 pm shorter than that of strontium. This result demonstrates that useful structure data for metal hydrides containing heavily absorbing elements can be obtained from neutron powder diffraction provided the experimental conditions are optimized and suitable structure refinement procedures are adopted. Nevertheless, high-resolution X-ray diffraction experiments remain essential to detect lattice distortions, and a combination of both techniques is usually the method of choice for obtaining reliable metal-hydrogen bond distances in metal hydrides. Finally, the structural characterization of the metal hydrides covered in this work were at the limit of present day technology and methodology, which underlines

the importance of advances in instrumentation and crystallographic methodology for solid-state research.

#### Acknowledgments

We thank Dr. P. Fischer (ETH Zürich and PSI, Villigen, Switzerland) for valuable discussions, and the staff of the powder diffractometers D20 and D4b at ILL, and of BM1B of the Swiss-Norwegian beamlines at the European Synchrotron Radiation Facility (all at Grenoble, France) for their experimental assistance.

Received: March 30, 2001

- [1] H. Kohlmann, F. Gingl, T. Hansen, K. Yvon, *Angew. Chem.* **1999**, *111*, 2145; *Angew. Chem. Int. Ed.* **1999**, *38*, 2029.
- [2] H. Kohlmann, K. Yvon, *J. Alloys Comp.* **2000**, *299*, L16.
- [3] H. Kohlmann, B. Bertheville, T. Hansen, K. Yvon, *J. Alloys Comp.* **2001**, to be published.
- [4] V.F. Sears, *Neutron News* **1992**, *3*, 26.
- [5] J.E. Lynn, *J. Appl. Crystallogr.* **1989**, *22*, 476.
- [6] D. Schmidt, B. Ouladdiaf, *J. Appl. Crystallogr.* **1998**, *31*, 620.
- [7] J. Rodriguez-Carvajal, FullProf, Version 3.1d, **1996**, ILL (unpublished); R.A. Young, A. Sakthivel, T.S. Moss, C.O. Paiva-Santos, *J. Appl. Crystallogr.* **1995**, *28*, 366.
- [8] A.C. Larson, R.B. Von Dreele, General Structure Analysis System (GSAS), Los Alamos National Laboratory Report LAUR 86-748, **2000**.
- [9] A.W. Hewat, *Acta Crystallogr. A* **1979**, *A35*, 248.
- [10] W.A. Dollase, *J. Appl. Crystallogr.* **1986**, *19*, 267.
- [11] N.E. Brese, M. O'Keeffe and R.B. Von Dreele, *J. Solid State Chem.* **1990**, *88*, 571.
- [12] H. Kohlmann, H.E. Fischer, K. Yvon, *Inorg. Chem.* **2001**, in press.
- [13] F. Gingl, K. Yvon, P. Fischer, *J. Alloys Comp.* **1994**, *206*, 73.
- [14] F. Gingl, K. Yvon, M. Zolliker, *J. Alloys Comp.* **1994**, *216*, L1.
- [15] F. Gingl, A. Hewat, K. Yvon, *J. Alloys Comp.* **1997**, *253*, 17.
- [16] F. Gingl, K. Yvon, P. Fischer, *J. Alloys Comp.* **1992**, *187*, 105.
- [17] F. Gingl, K. Yvon, T. Vogt, *J. Alloys Comp.* **1997**, *256*, 155.
- [18] F. Gingl, F. Bonhomme, K. Yvon, P. Fischer, *J. Alloys Comp.* **1992**, *185*, 273.
- [19] F. Gingl, K. Yvon, P. Fischer, *J. Alloys Comp.* **1993**, *201*, 105.
- [20] B. Bertheville, K. Yvon, *J. Alloys Comp.* **1999**, *288*, 197.
- [21] K. Kadir, D. Noréus, *Z. Physik. Chem.* **1993**, *179*, 243.
- [22] B. Bertheville, K. Yvon, *J. Alloys Comp.* **1999**, *290*, L8.
- [23] B. Huang, F. Gingl, K. Yvon, J. Rodriguez-Carvajal, *J. Alloys Comp.* **1995**, *227*, 131.